Geotechnical characteristics of a Rubber Intermixed Ballast System

Chathuri M. K. Arachchige
BSc (Hons)
PhD Candidate, Transport Research Centre, University of Technology Sydney, NSW 2007. Australia.
Email: chathuri.arachchige@student.uts.edu.au
ORCID ID: https://orcid.org/0000-0003-1554-6527

Buddhima Indraratna
PhD (Alberta), MSc (Lond.), BSc (Hons., Lond.), DIC, FTSE, FIEAust., FGS, CEng, CPEng
Distinguished Professor of Civil Engineering, Founding Director of Australian Research Council's Industrial Transformation Training Centre for Advanced Technologies in Rail Track Infrastructure (ITTC-Rail), Director of Transport Research Centre, School of Civil and Environmental Engineering, University of Technology Sydney, NSW 2007, Australia. Email: buddhima.indraratna@uts.edu.au
ORCID ID: https://orcid.org/0000-0002-9057-1514

Yujie Qi
PhD, MSc, BSc
Lecturer, and Program Co-leader of Transport Research Centre, School of Civil and Environmental Engineering, University of Technology Sydney, NSW 2007, Australia. Email: yujie.qi@uts.edu.au
ORCID ID: https://orcid.org/0000-0002-3486-2130

Jayan S. Vinod
PhD, M.Tech, B.Tech
Associate Professor, ARC Training Centre for Advanced Technologies in Rail Track Infrastructure (ITTC-Rail), University of Wollongong Australia, NSW 2522, Australia.
Email: vinod@uow.edu.au
ORCID ID: https://orcid.org/0000-0002-2611-3594

Cholachat Rujikiatkamjorn
PhD, MEng (AIT), BEng (Hons)
Professor, Transport Research Centre, School of Civil and Environmental Engineering, University of Technology Sydney, NSW 2007, Australia. Email: cholachat.rujikiatkamjorn@uts.edu.au
ORCID ID: https://orcid.org/0000-0001-8625-2839

*Author for correspondence:
Distinguished Prof. Buddhima Indraratna
School of Civil and Environmental Engineering,
Faculty of Engineering and Information Technology,
University of Technology Sydney,
Sydney NSW 2007, AUSTRALIA
Ph: +61 2 4221 3046, Email: buddhima.indraratna@uts.edu.au

ABSTRACT

This study aims to promote the concept of using rubber granules from waste tyres as elastic aggregates blended with traditional ballast particles for better performance of rail tracks, i.e. a Rubber Intermixed Ballast System (RIBS). This paper describes the mechanical and compressibility characteristics of RIBS under monotonic loads and a criterion designed to determine the optimum rubber content in the proposed RIBS. The most interesting findings of this study embrace how the rubber granules in the blended rockfill assembly significantly reduce the dilation and modulus degradation, and the breakage of ballast aggregates. RIBS with more than 10% of rubber demonstrates a seemingly consistent reduction in dilation under changing confining pressures. Increased deviator stress and larger effective confining pressure compress the rubber particles within the RIBS which may cause relatively large initial settlements in the ballast layer, if the rubber content becomes excessive. It is also evident from the results that rubber particles ranging from 9.5mm to 19mm with similar angularity to ballast aggregates are advantageous, because, they reduce the breakage of load-bearing larger aggregates, thus effectively controlling ballast fouling within the granular matrix.

Key words: Rubber intermixed ballast, Triaxial compression test, Ballast breakage, Modulus degradation

Declarations

Funding

The research leading to these results received funding from Australian Research Council Discovery Project (ARC-DP180101916) and ARC Industry Transformation Training Centre for Advanced Rail Track Technologies (ITTC-Rail IC170100006).

Conflicts of interest/Competing interests

The authors have no conflicts of interest to declare that are relevant to the content of this article.

Availability of data and material

Some or all data used during the study are available from the corresponding author by request (static triaxial test data).

Code availability (Not applicable)

Ethics approval (Not applicable)

1. Introduction

Ballasted railways are among the commonly used track infrastructure, as they provide adequate load bearing capacity and stability subjected to a large range of moving loads apart from ensuring rapid drainage. Despite these benefits, ballasted railways exhibit shortcomings that are mainly associated with track stability as the ballast becomes degraded over time. After a certain period of operation, damaged ballast can no longer be used, and requires replenishment with freshly quarried ballast which is one of the most expensive budget items in track maintenance schemes in Australia [17].

In recent years, researchers have been investigating a variety of approaches to utilise recycled industry wastes (i.e. tyre derivatives, coal wash, plastics, glass, etc.) in railway substructure to identify and evaluate sustainable and innovative ways of recycling various types of industrial wastes, while reducing track degradation and enhancing the performance. Different approaches have already been reported to a limited extent. For instance, Ho et al. [9] and Kennedy et al. [18] introduced a blended ballast matrix such as elastomeric particles bounded with the polymer matrix resin, and Fathali et al. [6] tested ballast mixed with tyre derived aggregates without a binder as an alternative to traditional ballast. Qi et al. [24] proposed the use of shredded or crumbed rubber blended with steel furnace slag and coal wash in sub-ballast. Moreover, Arulrajah et al. [1] introduced recycled plastic and demolition wastes as railway capping materials, while Naeini et al. [23] introduced recycled glass into these waste mixtures and evaluated stiffness and strength characteristics of capping layer.

Some previous studies [6, 27, 28] attempted to evaluate the impact of adding rubber granules in ballast employing uniaxial compression tests and direct shear tests under dynamic loading. The most notable findings to emerge from the literature imply that rubber added to a ballast assembly could reduce ballast breakage and damage to track elements by increasing the capacity of the ballast layer to retain more strain energy [6, 27]. The addition of rubber reduces the shear strength and stiffness of the ballast and increases its total settlement [28]. This is primarily attributed to the elastic modulus of rubber granules which are significantly lower than that of rock aggregates. In previous studies, the particle size distribution of rubber granules has generally followed the same shape of ballast gradations for compatibility of intermixing [4, 6, 28]. The study by Esmaeili et al. [5], investigated the dynamic properties of rail ballast mixed with tyre-derived aggregates (TDA) in a modal shaker test, and they found a significant decrease in overall stiffness associated with an increase in the damping ratio as the amount of TDA increased (e.g. 22% of TDA in the ballast mixture decreased the stiffness more than 90% and increased the damping ratio more than 60%). A follow-up study by the same author [4] found that 10% by volume of TDA could reduce the stiffness of pure ballast to one-fourth. This confirms that the overall behaviour of ballast and rubber mixtures is directly influenced by the rubber particles.

Some researchers [27] suggest mixing rubber granules that are considerably smaller than the ballast particle sizes (8mm-22.4mm), but this may not be a practical option, because, relatively smaller rubber particles can contribute to ballast fouling (void filling) and segregation rather than improving the energy absorbing capability of a well-interlocked matrix. M.Sol-Sanchez et al. [27] and Esmaeili et al. [5] suggested that 10% of rubber granules by volume could reduce ballast degradation and increase the capacity of the ballast to absorb energy and also maintain an acceptable level of stiffness of the matrix. Fathali et al. [6] proposed 10% by weight as a suitable amount of rubber granules based on the combined effects of physical and mechanical properties, while Gong et al. [7] and Guo et al. [8] also proposed the same recommendation of 10% by weight, considering particle breakage. Considering various available ballast standards, Song et al. [28] suggested the addition of about 5% of rubber particles by volume, in relation to the acceptable mechanical and damping properties expected of a high quality ballast.

All these experimental and numerical studies found in the literature so far have focused on the dynamic properties of railway ballast mixed with rubber granules, and they did not offer consistent and convincing explanations regarding the optimum amount or the size of rubber particles to be utilised. Since all these studies were conducted using either a ballast box, a direct shear test, or a modal shaker, none of the authors has considered the roles of stress ratio, modulus degradation, and the compression/dilatancy, response to changing confining pressures, when selecting the optimum amount of rubber. Furthermore, none of these studies took place in the triaxial space to evaluate the relevant behaviour during the shearing process.

In view of the above, this paper presents important insights of the behaviour of Rubber Intermixed Ballast System-RIBS using large-scale triaxial tests under three different effective confining pressures 10kPa to 60kPa where different weight percentages of rubber (R_b) ranges from 0-15%. A Particle size of rubber granules is proposed based on the minimal effect on stiffness degradation and ballast fouling. A stability-based parametric approach is used to evaluate the optimum amount of rubber in RIBS, while considering the geotechnical properties of RIBS, i.e. the shear strength, stiffness degradation, reduced dilation, energy absorption capacity, and ballast breakage.

2. Materials and testing program

2.1 Test material

Fresh ballast for this study was obtained from Bombo Quarry (New South Wales, Australia), and it consisted of latite basalt, which is widely used for railway tracks in the local region. Rubber granules were obtained from scrapped tyres by the standard shredding process. The maximum particle size of the ballast was limited to 53mm to ensure that the ratio of the diameter of the test specimen (300 mm) to the largest particle size is not less than 6, to avoid the boundary effect during triaxial testing [22]. The specific gravities of the ballast and rubber granules were 2.8 and 1.15, respectively. The target particle size distribution (PSD) curve of RIBS with different percentages of rubber granules along with the details such as the maximum (D_{max}) and minimum (D_{min}) particle sizes, the coefficient of uniformity (C_u), the coefficient of gradation (C_c) and the particle size distributuion of rubber granules are shown in Fig. 1. RIBS gradation is appropriate for use as a railway ballast according to the nominal 60 graded specifications specified by the latest Australian Standard (AS 2758.7:2015).

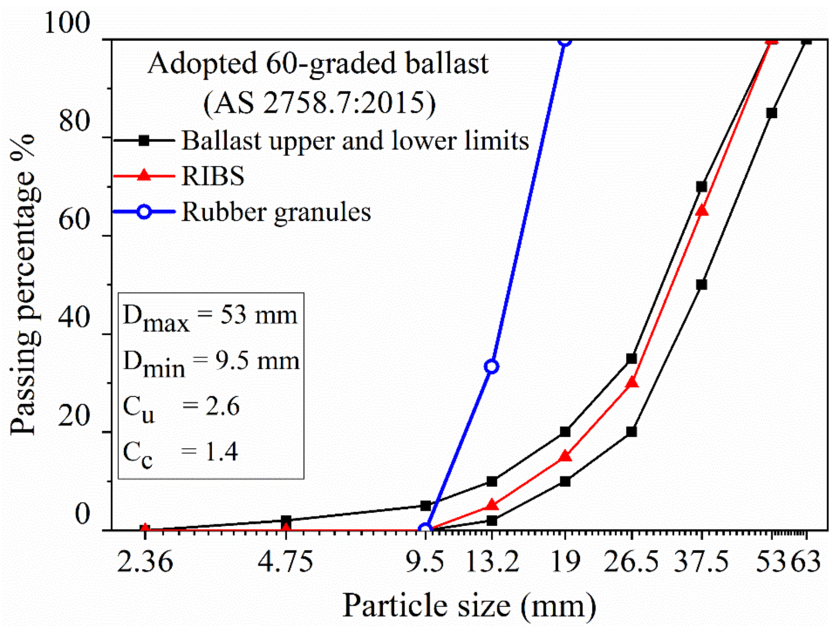

Fig. 1 Particle size distribution of RIBS and rubber granules

According to past experimental studies [10, 12] and the current laboratory tests conducted for commonly used ballast in the state of NSW in Australia (latite basalt), it is shown that larger ballast grains (19mm-53mm) are more susceptible to breakage than smaller particles. This is because bigger particles forming the skeleton of compacted ballast tend to be more angular, and consequently taking much of the applied stress concentrations [10]. Besides, Khoshoei et al. [19] did some experiments with steel slag aggregates with tyre derived aggregates and found that the specimens with larger rubber aggregates (20mm-60mm) were not as stiff as the samples with smaller rubber aggregates (10mm-20 mm). Moreover, the larger particles of scrapped tyre granules are too planar and flaky as a result of the shredding process, and may not be appropriate for a typical rail ballast mix (Fig. 2a). The elongated nature of the particles is different from the usual angular shape of the ballast, and therefore they cannot interlock properly. Furthermore, those rubber particles less than 9.5 mm can cause fouling without adding any favourable effects to RIBS. For this reason, the rubber granules used in this study range from 9.5mm to 19.5mm to maintain the structure of the ballast matrix without compromising its stiffness and shear strength. Fig. 2(b-d) shows the visual appearance of pure ballast, rubber granules and the rubber intermixed ballast used in this study.

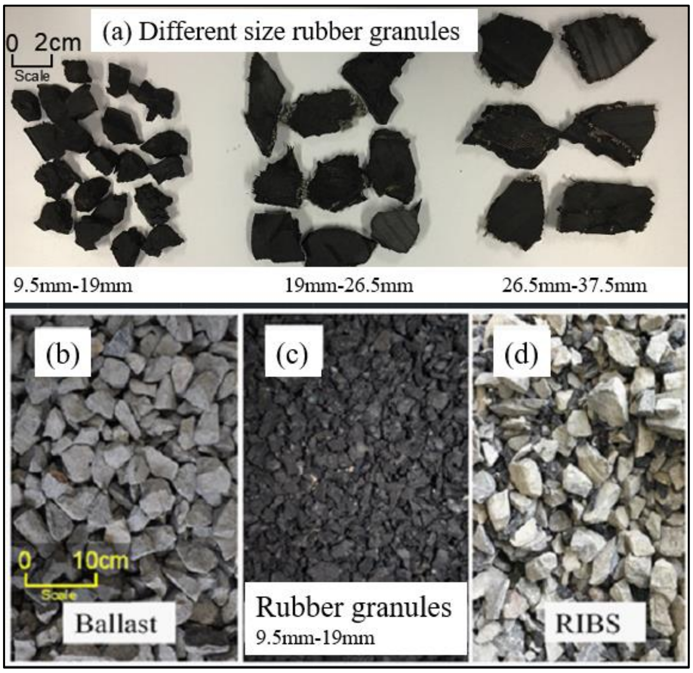

Fig. 2 (a) Shape of different size rubber granules; (b) Pure ballast; (c) rubber granules; (d) rubber intermixed ballast system (RIBS)

2.2 Triaxial test procedure

A series of triaxial tests were carried out on specimens of 300 mm in diameter and 600 mm in height using the large-scale triaxial apparatus. This apparatus consisted of a main chamber, a pressure control unit, a volume change measuring device, a loading actuator and a data logger, all of which were controlled by the fully automated servo-control unit. This apparatus enables a specimen to undergo triaxial loading under a constant effective confining pressure. A more detailed description of the test apparatus can be found in Indraratna et al. [10].

Fresh ballast was sieved, washed, dried and then mixed with a certain amount of rubber granules to achieve target PSD as shown in Fig. 1. This was carried out by pre-calculating the mass of each particle range while keeping the same initial void ratio of 0.824 the same as the pure ballast for all the specimens. The initial void ratio for compacted fresh ballast was achieved by tamping lightly to ensure minimum particle breakage while preparing the test specimens. The densities and the specific gravities of RIBS after compaction are given in Table 1. The specimens were compacted in four layers to reach the target initial void ratio, within the confinement of a 7 mm thick rubber membrane. Before testing, each specimen was saturated under a back pressure of 10kPa until Skempton's B value of at least 0.98 was reached. The target isotropic effective confining pressures (i.e., σ'_3 =10, 30 and 60kPa) were selected to represent the actual field conditions for conventional tracks [29]. Each specimen was subjected to axial strain up to 20-25% until they failed or reached the maximum axial strain limit of the apparatus. The applied shearing rate was 1.5mm/min, which was gradual enough to prevent any excess pore pressures building up to maintain drained condition. The stress measurements were corrected for the membrane effect as per ASTM D7181-20 [2]. After completing each test, the specimens were then sieved to determine the extent of ballast breakage. During testing, the shape and texture of the rubber aggregates prevented segregation within the compacted RIBS mixture.

Table 1 Initial specific gravity, density, relative density and the effective friction angle

R_b (%) in the RIBS mixture	Initial specific gravity	Density (kg/m^3)	Relative density, Dr %	Effective friction angle, φ_{ef}
0	2.8	1535	1.00	48.8
5	2.61	1432	0.93	48.4
10	2.45	1342	0.87	47.7
15	2.3	1263	0.82	46

3. Experimental results and discussion

3.1 Stress-Strain response

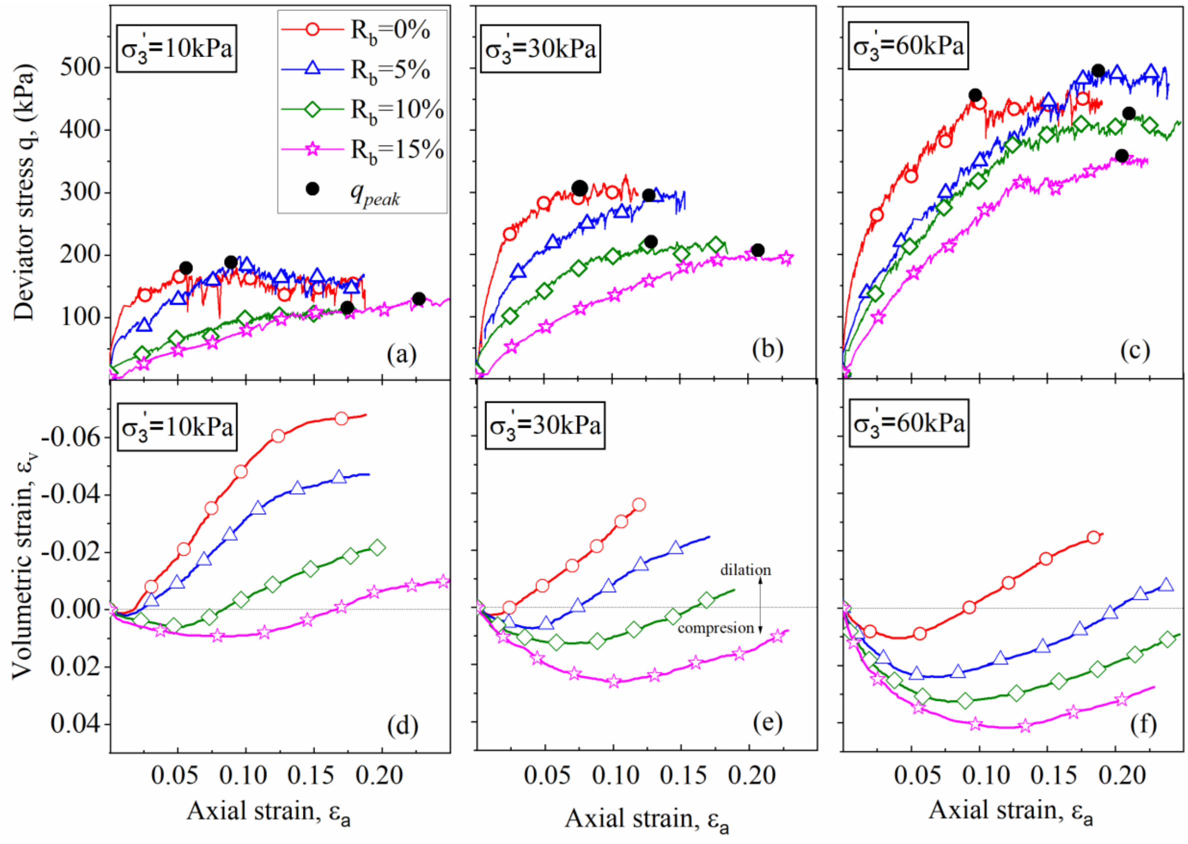

Fig. 3 Effect of the rubber on: (a-c) deviator stress-axial strain curves; (d-f) volumetric-axial strain curves

In this paper the conventional triaxial stress parameters: p' (mean effective stress) and q (deviator stress) are calculated from $p' = \frac{\sigma_1' + 2\sigma_3'}{3}$ and $q = \sigma_1'$-σ_3', where σ_1', and σ_3' are the principal effective compressive stresses. The volumetric strain (ε_v) can be determined from ($\varepsilon_a + 2\varepsilon_r$) where ε_a and ε_r are the axial and the radial strain, respectively. Typical stress-strain curves for RIBS mixtures with different R_b (i.e., 0%, 5%, 10% and 15%) at different effective confining pressures (i.e., σ'_3 =10, 30 and 60kPa) are shown in Fig. 3. Note that the deviator stress of all the specimens increases with the axial strain until they reach the peak deviator stress, and there is no pronounced strain-softening except for pure ballast and for the ballast with 5% rubber at $\sigma'_3 = 10$kPa. This complements the observations made earlier by Indraratna et al. [16] and Lackenby et al. [20], as failure of ballast is generally accompanied by bulging towards the centre of the specimen, rather than a distinct shear plane across the specimen. The computed peak deviator stress ratio (η_{peak}) has been denoted as a dark solid circle on each plot. Note that the peak deviator stress (q_{peak}) increases as the effective confining pressure increases, whereas under the same effective confining pressure, q_{peak} decreases with an increasing R_b when the amount of rubber is >5%. However, when R_b=5%, the RIBS mixtures have the relatively similar q_{peak} to pure ballast, but when the amount of rubber increases the RIBS mixtures exhibit a rubber-like behaviour (Fig. 3a-c) as they reach their peak stress at relatively higher axial strains, thus transforming the RIBS mixture from a brittle to a ductile state. Moreover, the volumetric strain of RIBS with R_b >5% barely stabilised by the end of the test, probably because the rubber particles continued to deform until the end of the test, thus preventing the volumetric strain to attain a constant value, i.e. a critical state.

Unlike the light tamping while preparing the test specimen, increased deviator stress and larger effective confining pressure compress the rubber particles in the RIBS mixtures and make notable changes in the compressive behaviour of the mix compared to pure ballast specimens (Fig. 3d-e). The rubber grains in a compressed state trigger effective particle interlocking (i.e., it reduces the volume of voids) to make the material denser than its initial state. Similar to the way in which an increased effective confining pressure would suppress volume expansion, an increased density reduced the volume compression, followed by dilation of the dense granular assembly as shearing progressed.

As shown in Fig. 3d-e, pure ballast and RIBS with 5% rubber (σ'_3<30kPa) show only limited initial volumetric contraction in contrast to overall dilation, whereas test specimens of RIBS with R_b>5% undergo significant initial compression before any dilation. RIBS with increased rubber content at larger effective confining pressures demonstrate larger compressions (e.g. 4% for RIBS with 15% rubber at effective confining pressure, $\sigma'_3 = 60$kPa) which may cause relatively large initial settlements in the ballast layer. A closer inspection of Fig. 3a-c shows that some abruptly fluctuating undulations in the otherwise relatively smooth stress-strain curves represent ballast breakage or attrition of rough and angular surfaces of coarse particles during shearing (slipping). It is noted that these erratic undulations become insignificant as the percentage of rubber increases, which indicates reduced ballast breakage within the granular assembly. This may be attributed to an increase in contact surface area between ballast and rubber (i.e. better interlock) which resist slipping and alleviate to some extent the high stress concentrations at particle contacts.

3.2 Modulus degradation

The stress-strain plots in Fig. 3a-c follow the typical stress-strain behaviour for loose sand. To obtain the initial tangent modulus, this typical stress-strain behaviour was approximated by the hyperbolic stress-strain curve [3] as shown in Fig. 4a and given by the following equation.

$$q = \frac{\varepsilon_{\mathrm{a}}}{a + b\varepsilon_{\mathrm{a}}} \tag{1}$$

where a and b are model parameters determined by curve fitting the experimental data (R^2>0.98).

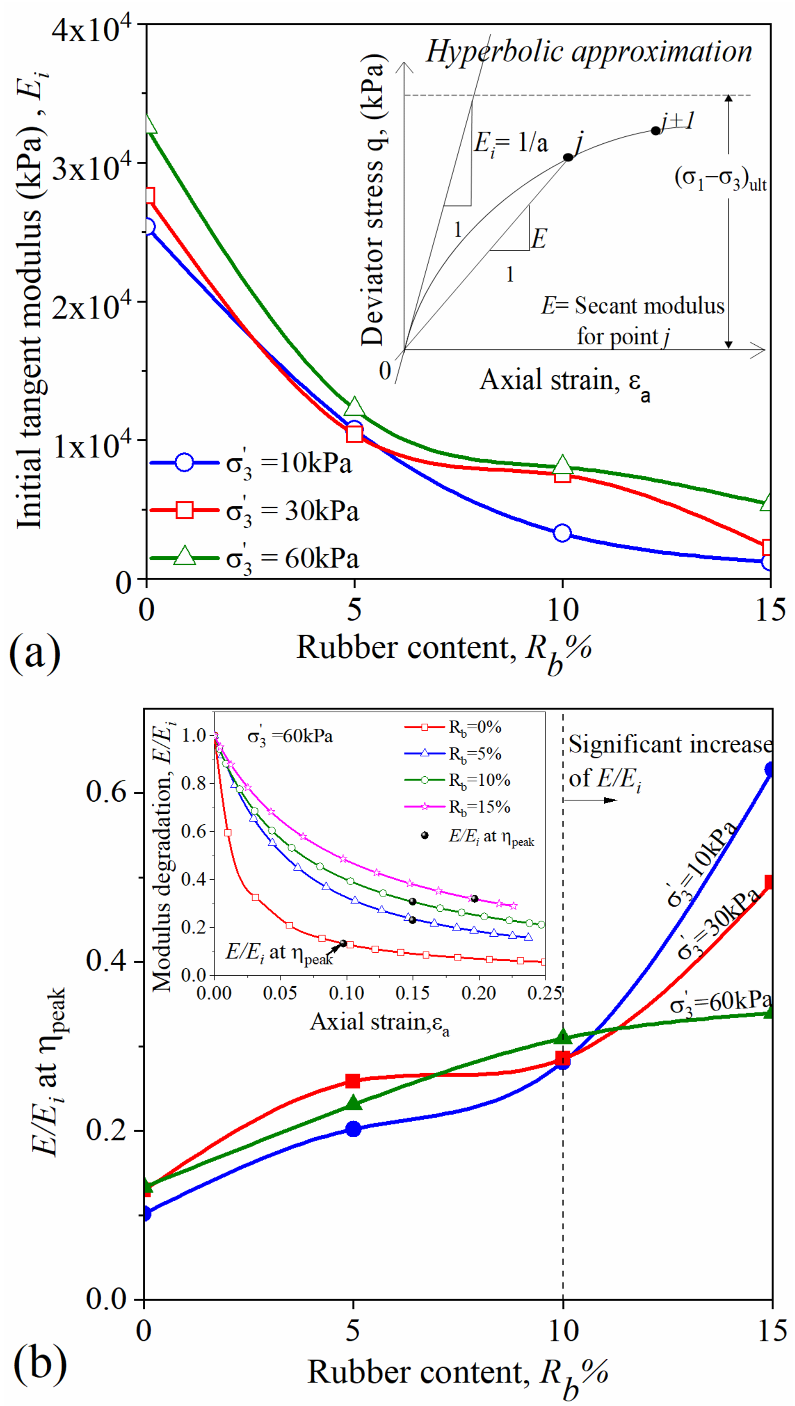

Fig. 4 (a) Initial tangent modulus of RIBS; (b) secant modulus degradation of RIBS at η_{peak}. Note an insert shows the variation of secant modulus degradation with axial strains at confining pressure of 60 kPa

In Fig. 4a, based on the hyperbolic fit, $1/a$ is the initial tangent modulus E_i and $1/b$ is the ultimate principal stress difference. The secant modulus of soil (E), is defined as the ratio between the difference in deviator stress to the corresponding axial strain, where E=$\Delta q/\Delta\varepsilon_{\text{a}}$. Modulus degradation at a point is determined by the ratio, E/E_i. The initial tangent modulus E_i, represents the short-term static modulus of elasticity which is required to calculate the initial elastic track settlements. It is also a good indicator of the ductility of the materials because a lower E_i means higher ductility. In Fig. 4a there is a clear trend of decreasing E_i with the introduction of rubber into the mixture, thus indicating reduced stiffness and increased ductility. Under the same confining pressure when R_b = 5%, the reduction of E_i is around 60% comparing to pure ballast. Any further increase in the amount of rubber in the RIBS tends to have a lesser influence on further reducing the value of E_i. It is also clear that for the specimens with the same rubber content, an increase in the effective confining pressure increases the value of E_i. The modulus degradation at η_{peak} is shown in Fig. 4(b), where η_{peak} is the peak stress ratio obtained by determining the maximum stress ratio (η) based on the η-ε_a plot. The modulus degradation (E/E_i) rapidly decreases and attains stability in pure ballast, but an increase in the amount of rubber in the RIBS mixtures slows down the rate of modulus degradation (Fig. 4b). Therefore, for the RIBS samples with increased rubber (R_b>10%), the modulus degradation is notable, even at the large axial strains (ε_a>0.15). The reason for this gradual decrease in the rate of modulus degradation (shape of modulus degradation curve) can be attributed to the increased particle interlocking due to the deformation of rubber granules. RIBS materials with increased rubber can undergo significant axial deformation before failure compared to pure ballast. In other words, the reduced rate of modulus degradation increases the failure strain, i.e. increased ductility. For instance, at $\sigma'_3 =$ 60kPa the axial strain at peak stress ratio (where E/E_i starts stabilizing) increases from 0.09 to 0.2 when R_b increases from 0 to 15%. Therefore, due to the increased ductility, the value of E/E_i at peak stress ratioincreases with the increased rubber content (Fig. 4b). However, when R_b increases to 15% a sharp increase in E/E_i is observed. Note also, when R_b>10%, the influence of confining pressure on the E/E_i becomes pronounced, and E/E_i reduces as σ'_3 increases.

3.3 Friction angle and dilation angle

The internal friction of ballast material governs the stability of the track. Previous studies [14, 26] reveal that the effective friction angle (φ_{ef}) of fresh ballast varies from 46° to 69°as the effective confining pressure increases from 10kPa to 300kPa. However, it can be a challenging task to obtain a RIBS mixture without reducing its shear strength attributed to the lower strength of rubber compared to intact rock aggregates, hence the importance of ensuring the ideal or optimum rubber content in the mix. For instance, Song et al. [28] showed that a mixture of ballast and rubber with the same gradation (R_b=10%) significantly reduces the internal friction angle of ballast (by 24%). The effective friction angle of RIBS mixtures in this study was calculated using the peak deviator stresses, and tabulated in Table 1. Note that increasing R_b from 0 to 15% led to a minor change in the effective friction angle for RIBS mixtures from 48.8° to 46.0°. This indicates that replacing the typical size range of ballast between 9.5 to 19.5mm with up to 15% of rubber granules may have only marginally compromised a reduction in the overall shear strength.

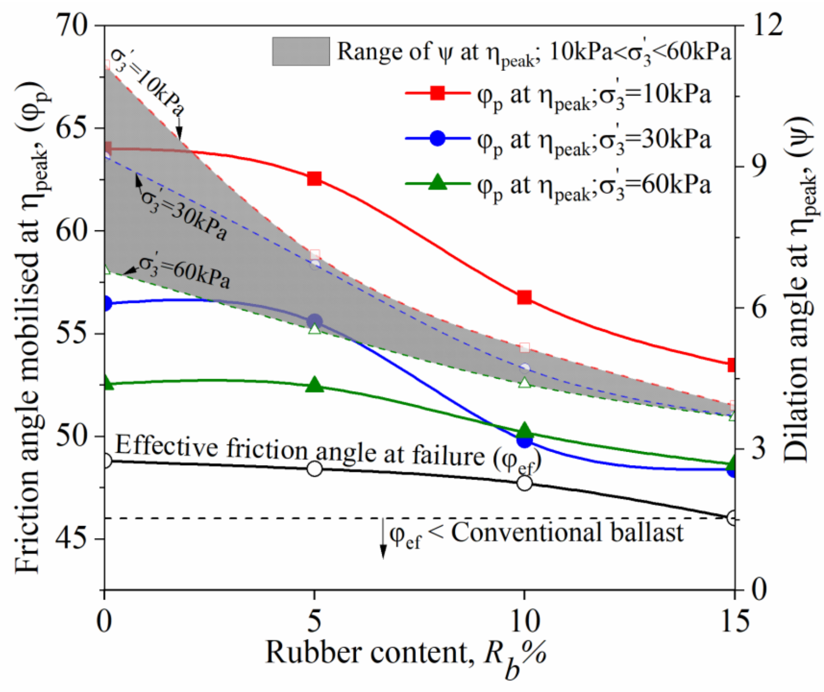

Fig. 5 Effect of the rubber on effective friction angle φ_{ef}, friction angle at peak stress ratio φ_p and the dilation angle (ψ)

The mobilised friction angle of all the specimens at the peak stress ratio (φ_p) was also determined and plotted against the percentage of rubber (Fig. 5). The mobilised friction angle at the peak stress ratio incorporates the effect of breakage and dilatancy of the sample thus corresponding to the stresses at peak stress ratio, whereas the effective friction angle (φ_{ef}) does not [12]. It can be seen that the difference between the φ_p and the φ_{ef} decreases as the amount of rubber increases; this represents reduced dilation and breakage. The dilation angle (ψ) is calculated using the equation $\sin\psi = -\frac{d\varepsilon_v/d\varepsilon_a}{2-d\varepsilon_v/d\varepsilon_a}$ where $d\varepsilon_v$ is the increment of volumetric strain and $d\varepsilon_a$ is the increment of axial strain. As also shown in Fig. 5, the dilation angle decreases as the amount of rubber increases and when R_b >5%, ψ of RIBS is less than that of conventional ballast; ψ decreases as the confining pressure increases and the effect of confining pressure is suppressed by the increased rubber content. This is clearly reflected by the plots for dilatancy $d = d\varepsilon_v/d\varepsilon_a$ versus stress ratio shown in Fig. 6 and further explained below.

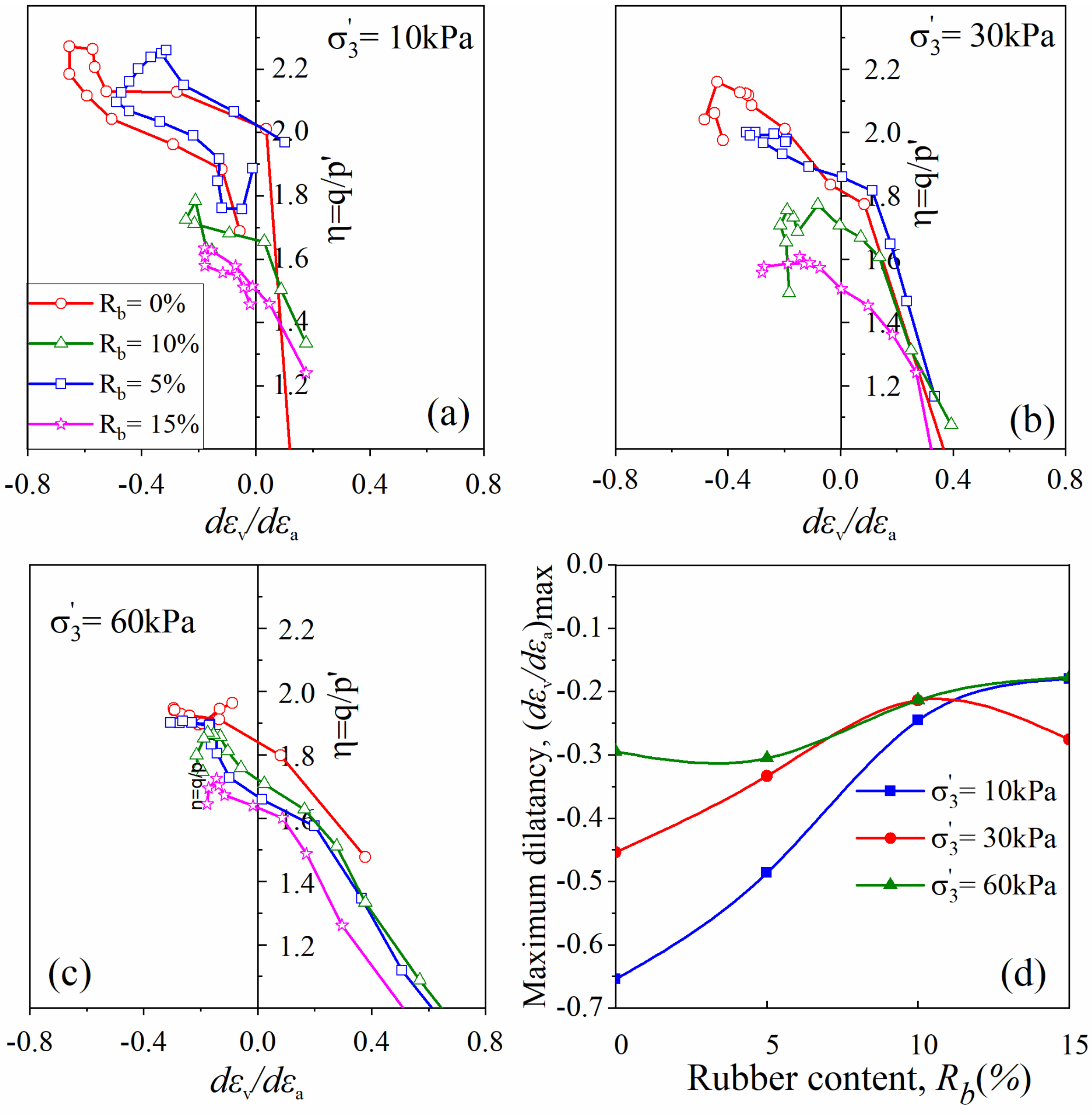

Fig. 6(a-c) Dilation-stress ratio responses of RIBS under different effective confining pressures: (a) 10 kPa, (b) 30 kPa and (c) 60 kPa; (d) Maximum dilatancy with rubber content

Fig. 6(a-c) shows that the peak stress ratio decreases as the confining pressure increases for conventional ballast and RIBS with R_b=5%. However, when R_b>5%, the change in the confining pressure shows an insignificant effect on the peak stress ratio and dilatancy of RIBS. The reason for this can be attributed to the induced rubber contracting during the initial shearing stage (up to $d\varepsilon_v/d\varepsilon_a$=0 for the first time) which then influences the stress-dilatancy behaviour more than the change in effective confining pressures (10kPa to 60kPa). Having a broadly similar stress-dilation behaviour with changing effective confining pressures is an advantage for RIBS mixtures (R_b>5%) in terms of controlling the lateral misalignments along the track in a practical perspective. However, while an increase in the amount of rubber decreases the peak stress ratio, this difference is not as significant under higher effective confining pressures (e.g. 60kPa). It is observed that the maximum dilatancy generally decreases with the increased rubber content, and the effect of confining pressure on dilatancy is insignificant when R_b>10% (Fig. 6(d)).

3.4 Ballast breakage

Ballast breakage is one of the key factors that cause track degradation. The particle breakage of RIBS mixtures has been quantified using the ballast breakage index (BBI) [13] and the classical particle breakage index (B_g) [21]. The definition of BBI is shown in Fig. 7a where the initial and final grading curves are needed during the calculations. B_g is the difference in the percentage of the weight of particles retained on the sieve before and after the test, i.e. $B_g = \Delta W_k = W_{ki} - W_{kf}$, where W_{ki} represents the percentage retained on sieve size k before the test and W_{kf} is the percentage retained on the same sieve size after the test. B_g is expressed as a percentage. BBI is a parameter that can be conveniently used to examine the overall particle breakage of the RIBS, while Marsal's breakage index B_g can demonstrate the sizes of ballast particles that are more prone to breakage and how the addition of rubber can control breakage for each particle size range. It has been found that if the BBI<0.1, then the breakage can be considered negligible [11].

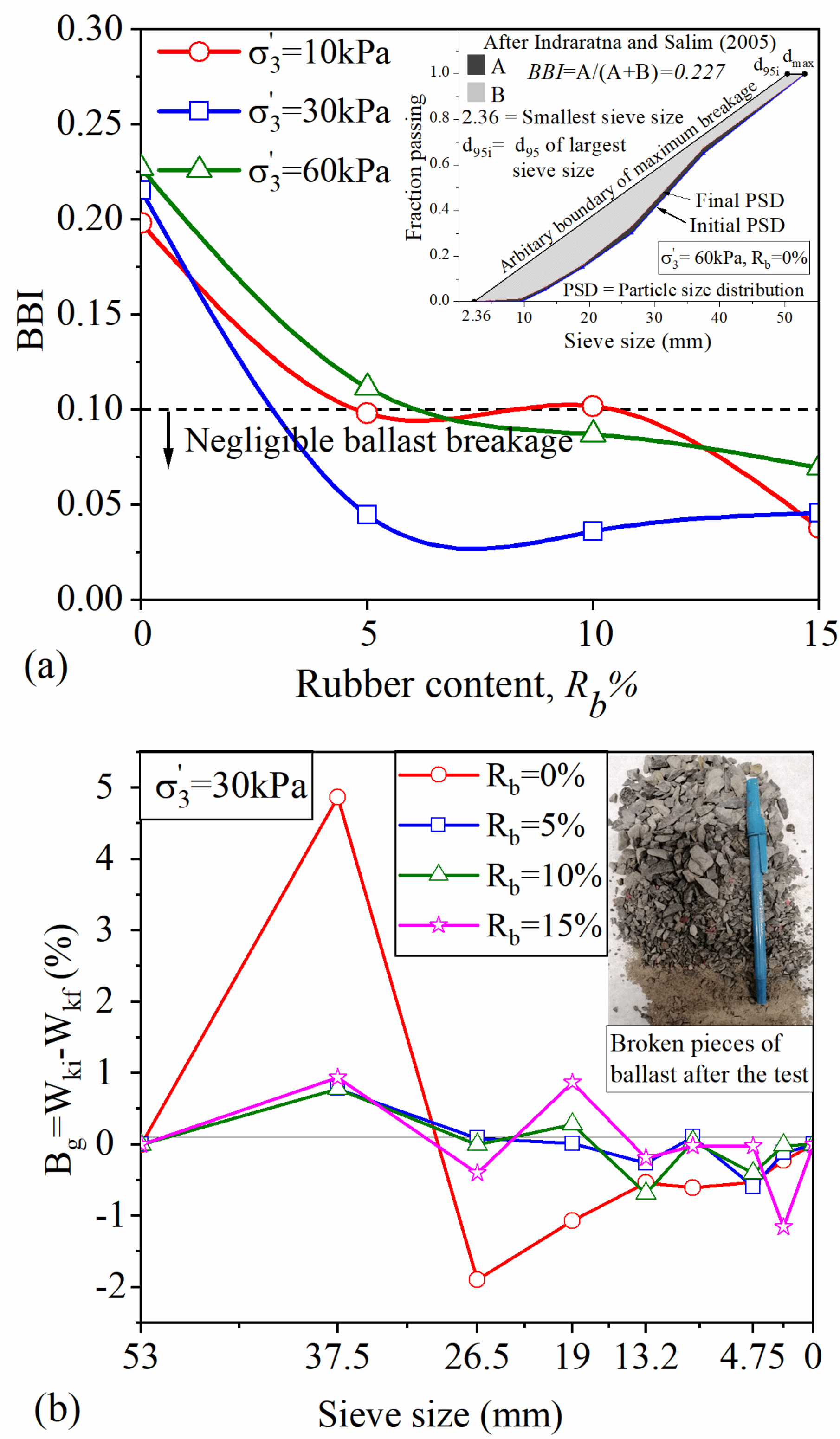

Fig. 7 Influence of R_b on: (a) ballast breakage index (BBI); (b) Marsal's breakage index, $B_g = \sum (\Delta W_k > 0)$

Fig. 7a shows the BBI of RIBS mixtures varying with R_b. A considerable amount of breakage (BBI=0.15-0.23) is found for pure ballast specimens under $\sigma'_3 = 10, 30$ and 60kPa; this agrees with previous studies by Indraratna and Salim [13] and Indraratna et al. [15]. The investigations of BBI in RIBS mixtures demonstrate negligible ballast breakage (BBI<0.1) after adding 5% or more of rubber. The change in B_g with the percentage of rubber in each RIBS mixture under an effective confining pressure of 30kPa is shown in Fig. 7b. There is more than 70% reduction in breakage in the larger ballast particles (>38mm) in all the specimens with rubber (irrespective of R_b) compared with pure ballast. A small increase in the amount of rubber enhances the internal stress distribution with an increased damping effect, and this significantly reduces the degradation of the larger particles. In this study, it is observed visually and after the sieve analysis for pure ballast, that corner breakage of highly angular particles contributed more to ballast degradation than splitting (i.e. across the body of the particles). The other possible reason for reduced ballast breakage in RIBS is the reduced angular corner breakage due to the increased contact areas between the ballast and rubber within the blended matrix (Fig. 7b). These observations seem to support the idea of replacing ballast with rubber granules in the size range of 9.5mm-19mm rather than larger sizes (>19mm), not only to preserve the strength of the material but also to reduce ballast breakage.

3.5 Energy absorption

To evaluate the energy absorption capacity of the RIBS mixture, the strain energy density (E_d) is used herein:

$$\mathrm{E}_d = \int_0^{\gamma f} \tau d\gamma \tag{2}$$

where γ_f is the shear strain up to the peak shear stress and τ is the shear stress; here $\tau = q/2$ and the shear strain is $\gamma = 3\varepsilon_q/2$. Here ε_q is the deviator strain where $\varepsilon_q = \varepsilon_\mathrm{a} - \varepsilon_v/3$.

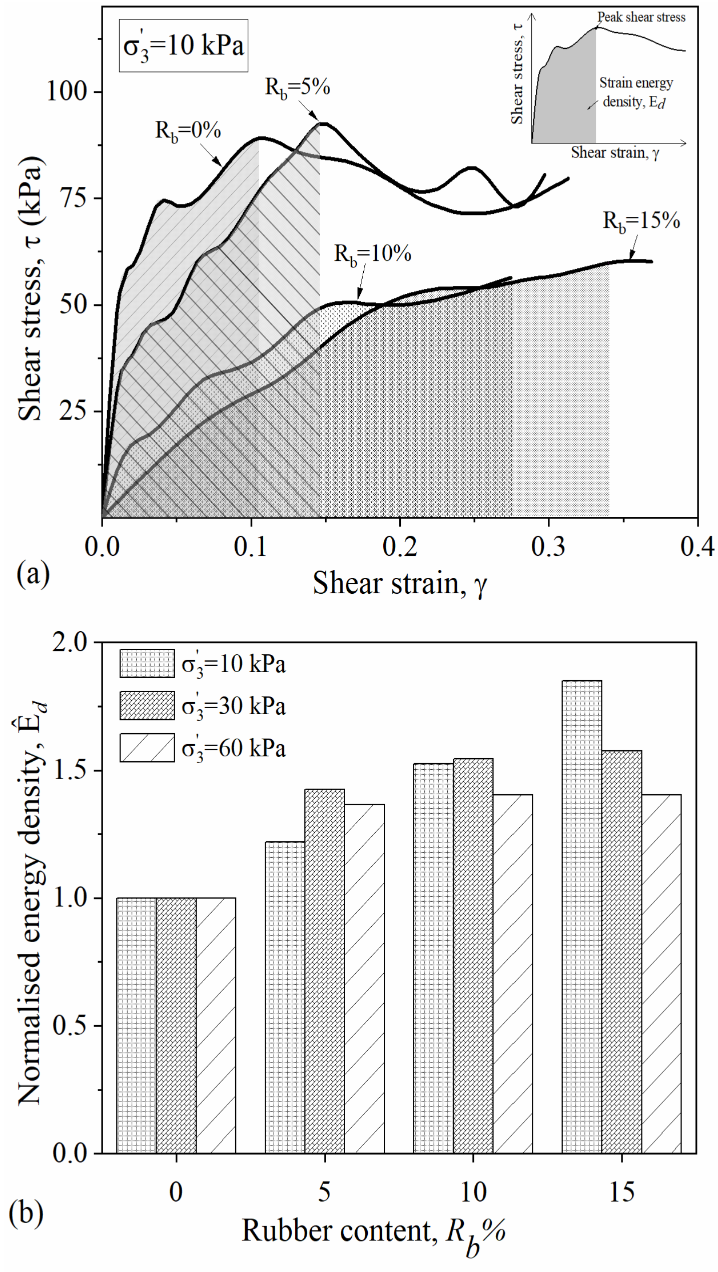

Fig. 8 (a) Shear strain versus shear stress; σ_3' =10kPa; (b) normalized strain energy densities variation against the rubber content

Fig. 8a shows the shear stress–strain plots for RIBS under effective confining pressures of 10kPa. In Fig. 8a, the points at which the shear stresses become stable (approaching a constant value) taken as the peak shear stress point. It can be seen the shaded area under the shear stress-strain curve up to the peak shear stress point increases as more rubber is added, meaning E_d increases under $\sigma'_3 = 10$kPa. To better evaluate the energy absorbing capacity of RIBS by adding rubber, a dimensionless ratio representing the normalised strain energy density $\hat{E}_d$ is proposed, namely the amount of absorbed energy density with respect to pure ballast. $\hat{E}_d$ is calculated for all specimens and shown in Fig. 8b. Note that the inclusion of rubber increases $\hat{E}_d$, indicating the energy absorption capacity of RIBS increases, which is because more energy is consumed during the contraction of highly compressible mixtures. The increase is more pronounced under low confining pressures (e.g. σ'_3 =10kPa to 30kPa). This is more favorable as the ballast layer in the field is normally subjected to only a very low confining pressure in the range 10kPa to 30kPa [14]. This is a justifiable reason for adding rubber to ballast materials meaning that the increased energy absorbing capacity of the ballast layer not only decreases ballast breakage internally, it also reduces the amount of energy transferring to other substructure layers (e.g. subballast and subgrade), hence reducing damage to overall track elements [25].

4. Proposed acceptance criteria for RIBS

In this paper, a design criterion is introduced to assess the optimum amount of rubber in a RIBS mixture considering the effective friction angle, dilatancy angle, ballast breakage, as well as energy absorption and modulus degradation at peak deviator stress ratio. Five levels of acceptance are proposed herein to determine the optimum amount of rubber in the RIBS, while aiming towards a reasonably steady condition over the long term.

Step 1: Frictional shear strength and dilation angle,

The effective friction angle (φ_{ef}) is one of the governing factors used to determine the bearing capacity of the ballast layer and the dilation angle (ψ) represent the dilation of the ballast. It is expected the RIBS with the optimal rubber content should have φ_{ef} not less than pure ballast $46° \sim 55°$ [14, 26], while ψ of RIBS is to be less than that of ballast to ensure controlled dilation.

Step 2: Axial strain at peak stress ratio

From the laboratory test data it is identified that the axial strain of pure ballast at peak stress ratio is around 0.1 under typical track confining pressures; σ'_3 =10kPa to 30kPa [16]. To avoid the consequences of excessive settlements of RIBS compared to the conventional ballast material, an axial strain of 0.1 at peak stress ratio is considered as the tolerable limit for RIBS design criteria under the same confining pressures of 10kPa to 30kPa.

Step 3: Ballast breakage

The proposed RIBS with rubber should present superior performance in terms of ballast breakage, so the BBI values of RIBS should not exceed the BBI values of pure ballast under the same confining pressures (0.2-0.22; Fig. 7a). Furthermore, it is highly possible that the addition of rubber can reduce the BBI significantly and the

RIBS can achieve negligible particle breakage (BBI=0.1) under possible track confining pressures up to 60kPa. Therefore, here a stricter criterion is adopted as BBI<0.1 for the selected RIBS.

Step 4: Modulus degradation

In traditional ballast, the rate of modulus degradation rapidly decreases with axial strain and then stabilise at a low value (0.1-0.12). However, an increase in the amount of rubber in the RIBS mixtures slows down the rate of modulus degradation, indicating higher ductility and the potential of RIBS to withstand failure at larger axial strains. In fact, it is important to ensure that the RIBS should have improved ductility than the pure ballast, hence the E/E_i at η_{peak} is expected to be over 0.12 and that is satisfied by all the RIBS samples.

Step 5: Energy density

It is suggested that the proposed RIBS should satisfy normalised strain energy density $\hat{E}_d > 1$ to ensure the energy absorbing capacity of RIBS material is larger than that of pure ballast to help minimize ballast degradation and ensure less energy being transmitted to the adjoining substructure layers.

5. Optimising the amount of rubber

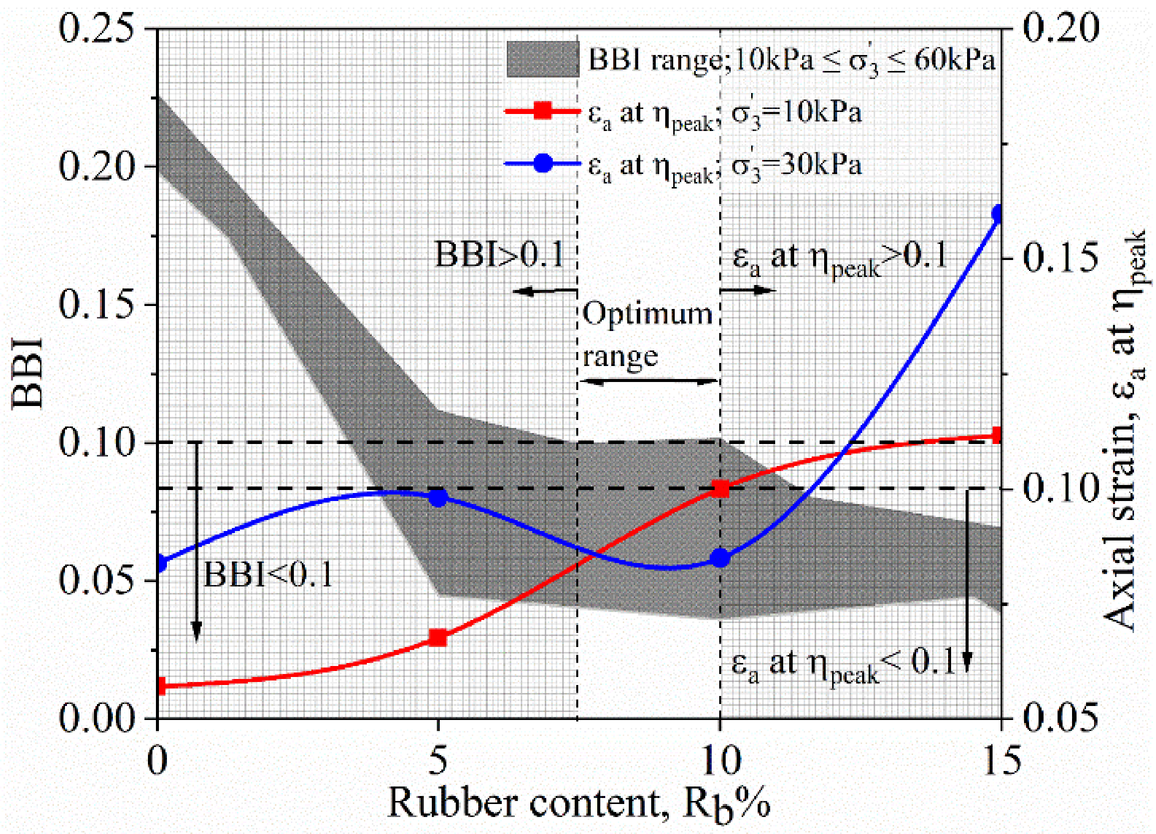

Fig. 9 Optimisation of rubber content

Using the proposed design criteria, the optimum amount of rubber in the RIBS mixture can be assessed as shown in Fig. 9, which shows how the optimum mixture is justified according to the ballast breakage index and the associated axial strain. When $R_b \geq 7.5\%$ all RIBS will present a negligible ballast breakage, i.e. BBI ≤0.1. Moreover, when R_b ≥10%, the axial strain at η_{peak} of RIBS will exceed the acceptable limit of 0.1 under the effective confining pressure 10kPa to 30kPa. Therefore, combining the test results of BBI and ε_{a} at η_{peak}, the acceptable range of rubber should be $7.5\% \leq R_b \leq 10\%$.

Moreover, all the RIBS samples show greater energy absorption capacities, reduced dilation angle and greater E/E_i at η_{peak} compared to the traditional ballast material. Also, the effective friction angle of RIBS with up to 15% of rubber is within the general range of pure ballast. Therefore, combining the selection result from Fig. 9, under possible real-life confining pressures (10kPa$<\sigma_3'<$30kPa) the optimum percentage of rubber in the RIBS can be prescribed confidently as 10% by weight, based on the findings of this study.

6. Conclusions

This paper has reported a study of the geotechnical properties of mixtures of ballast and rubber granules, i.e. Rubber Intermixed Ballast System (RIBS). A series of large scale static triaxial tests was carried out on RIBS with different amounts of rubber content (0-15%) and at effective confining pressures of 10, 30 and 60kPa. To ensure that the specimens of RIBS experienced less ballast breakage and dilation while preventing fouling, rubber shreds from 9.5mm to 19mm were used in lieu of the same size fraction of the natural ballast aggregates. The following salient findings could be drawn from this research:

- Overall, the current test results revealed that the inclusion of rubber increased the axial strain, the compressive volumetric strain, and the energy-absorbing capacity, while decreasing the dilation and ballast breakage. To optimise these mechanical properties and deformation characteristics without making the blended mix overly compressive, an optimum amount of 10% of rubber by weight could be recommended in the RIBS. The inclusion of rubber offered a significant reduction in ballast breakage, with more than 70% reduction in breakage of the coarser ballast particles (>38mm) in all the RIBS mixtures.
- Under the same effective confining pressure, the peak deviator stress, q_{peak} of RIBS decreased with an increasing amount of rubber >5%, however, this reduction in strength (i.e. drop in q_{peak}= 27% and 34% for RIBS with R_b =10% and 15% at σ_3' =30kPa) was certainly tolerable in relation to the obvious benefits of having less particle breakage.

- RIBS with an increased amount of rubber at larger effective confining pressures initially demonstrated larger volumetric contraction, however, the increased amount of rubber reduced dilation significantly compared to that of pure ballast, thereby improving track stability in a real-life perspective.
- The modulus degradation declined gradually as the amount of rubber was increased up to the optimum of 10% by weight, and the mix was stable at larger axial strains. This implies that the rubber contributes to increased ductility of the mix, hence in reality the track is expected to be more resilient while attaining a stable settlement.
- There was only a minor reduction of the effective friction angle (<6%) of the RIBS mixtures when the amount of rubber increased from 0 to 15%. This was mainly because the rubber fraction (9.5-19 mm) was of the same size and similar angularity of the replaced natural rockfill fraction. The decreased angle of shearing resistance could be attributed to the reduced particle hardness and surface roughness of the rubber particles compared to quarried natural rock aggregates.
- When $R_b \geq 10\%$, RIBS showed a similar stress-dilation behaviour with the increasing effective confining pressure, while indicating at least a 50% reduction in the dilation angle compared to pure ballast at confining pressures, $\sigma_3' \geq$30kPa.
- An increase in the amount of rubber by 10% increases the strain energy density of RIBS by around 15% in contrast to pure ballast, with the benefit of absorbing the energy transferred to the substructure, thus reducing track deterioration. At larger confining pressures ($\sigma_3' \geq$60kPa) the strain energy density is likely to remain steady with the increase of rubber more than 5%.

In summary, the findings of this study provide a perception of enhancing track longevity by reducing track degradation hence reducing the maintenance cycles over the period of track operation. At the same time, RIBS provides a solution for non-biodegradable waste material from the tyre industry at a low cost by reusing as an aggregate in railways while preserving the natural landscapes.

Acknowledgements

The authors would like to acknowledge the financial assistance provided by the Australian Research Council Discovery Project (ARC-DP180101916) and ARC Industry Transformation Training Centre for Advanced Rail Track Technologies (ITTC-Rail IC170100006). The Authors also acknowledge Bridgestone cooperation and Tyrecycle Australia for supplying rubber materials for the study.

References

1. Arulrajah A, Naeini M, Mohammadinia A, Horpibulsuk S, Leong M (2020) Recovered plastic and demolition waste blends as railway capping materials. Transp Geotech 22. https://doi.org/10.1016/j.trgeo.2020.100320
2. ASTM (2020) Methods for consolidated drained triaxial compression test for soils. ASTM D7181. West Conshohocken, PA: ASTM
3. Duncan JM, Chang CY (1970) Nonlinear analysis of stress and strain in soils. Soil Mech Found Eng
4. Esmaeili M, Ebrahimi H, Sameni MK (2018) Experimental and numerical investigation of the dynamic behavior of ballasted track containing ballast mixed with TDA. Proc Inst Mech Eng Part F: J Rail Rapid Transit 232(1):297-314. https://doi.org/10.1177/ 0954409716664937
5. Esmaeili M, Zakeri JA, Ebrahimi H, Sameni MK (2016) Experimental study on dynamic properties of railway ballast mixed with tire derived aggregate by modal shaker test. Adv Mech Eng 8(5):1-13. https://doi.org/10.1177/1687814016640245
6. Fathali M, Nejad FM, Esmaeili M (2016) Influence of tire-derived aggregates on the properties of railway ballast material. J Mater Civ Eng 29(1). http://dx.doi.org/0.1061/(ASCE)MT.1943-5533.0001702
7. Gong H, Song W, Huang B, Shu X, Han B, Wu H, Zou J (2019) Direct shear properties of railway ballast mixed with tire derived aggregates: Experimental and numerical investigations. Constr Build Mater 200:465-473. https://doi.org/10.1016/j.conbuildmat.2018.11.284
8. Guo Y, Markine V, Qiang W, Zhang H, Jing G (2019) Effects of crumb rubber size and percentage on degradation reduction of railway ballast. Constr Build Mater 212:210-224. https://doi.org/10.1016/j.conbuildmat.2019.03.315
9. Ho CL, Humphrey D, Hyslip JP, Moorhead W (2013) Use of Recycled Tire Rubber to Modify Track–Substructure Interaction. Transp Res Rec 2374:119-125. https://doi.org/10.3141/2374-14
10. Indraratna B, Ionescu D, Christie HD (1998) Shear behaviour of railway ballast based on large-scale triaxial tests. J Geotech Geoenviron Eng 124(5):439-449. https://doi.org/10.1061/(ASCE)1090-0241(1998)124:5(439)
11. Indraratna B, Ngo T (2018) Ballast railroad design: smart-uow approach. CRC Press, UK
12. Indraratna B, Salim W (2002) Modelling of particle breakage of coarse aggregates incorporating strength and dilatancy. Proc Inst Civ Eng Geotech Eng 155(4):243-252. https://doi.org/10.1680/geng.2002.155.4.243
13. Indraratna B, Salim W (2005) Mechanics of ballasted rail tracks: a geotechnical perspective. CRC Press, UK

14. Indraratna B, Salim W, Rajikiatkamjorn C (2011) Advanced rail geotechnology: Ballasted track. CRC Press, Rotterdam, Netherlands.

15. Indraratna B, Sun Q, Nimbalkar S (2015) A critical state based constitutive model for the triaxial response of ballast incorporating particle breakage. Proc XV Panamerican Conf on Soil Mech and Geotech Eng 1232-1239. http://dx.doi.org/10.3233/978-1-61499-603-3-1232

16. Indraratna B, Sun QD, Nimbalkar S (2015) Observed and predicted behaviour of rail ballast under monotonic loading capturing particle breakage. Can Geotech J 52:73-86. http://dx.doi.org/10.1139/cgj-2013-0361

17. Indraratna B, Tennakoon N, Nimbalkar S, Rujikiatkamjorn C (2013) Behaviour of clay-fouled ballast under drained triaxial testing. Géotechnique 63(5):410-419. https://doi.org/10.1680/geot.11.P.086

18. Kennedy J, Woodward P, Medero G, Banimahd M (2013) Reducing railway track settlement using three-dimensional polyurethane polymer reinforcement of the ballast. Constr Build Mater 44**:**615-625. https://doi.org/10.1016/j.conbuildmat.2013.03.002

19. Khoshoei SM, Bak HM, Abtahi SM, Hejazi M, Shahbodagh B (2021) Experimental Investigation of the Cyclic Behavior of Steel-Slag Ballast Mixed with Tire-Derived Aggregate. J Mater Civ Eng 33:04020468. https://doi.org/10.1061/(ASCE)MT.1943-5533.0003586

20. Lackenby J, Indraratna B, Mcdowell G, Christie D (2007) Effect of confining pressure on ballast degradation and deformation under cyclic triaxial loading. Ge´o-technique 57(6):527–536. https://doi.org/10.1680/geot.2007.57.6.527

21. Marsal RJ (1967) Large-scale testing of rockfill materials. Soil Mech Found Div 93(2)**:**27-43. https://doi.org/10.1061/JSFEAQ.0000958

22. Marschi ND, Chan CK, Seed HB (1972) Evaluation of properties of rockfill materials. Soil Mech Found Div 98(1)**:**95-114. https://doi.org/10.1061/JSFEAQ.0001735

23. Naeini M, Mohammadinia A, Arulrajah A, Horpibulsuk S, Leong M (2019) Stiffness and strength characteristics of demolition waste, glass and plastics in railway capping layers. Soils Found 59(6):2238-2253. https://doi.org/10.1016/j.sandf.2019.12.009

24. Qi Y, Indraratna B (2020) Energy-Based Approach to Assess the Performance of a Granular Matrix Consisting of Recycled Rubber, Steel-Furnace Slag, and Coal Wash. J Mater Civ Eng 32(7):04020169. https://doi.org/10.1061/(ASCE)MT.1943-5533.0003239

25. Qi Y, Indraratna B, Tawk M (2020) Use of Recycled Rubber Elements in Track Stabilisation. Proc Geo-Congress 2020 conf 49-59. Reston: American Society of Civil Engineers

26. Salim W (2004) Deformation and degradation aspects of ballast and constitutive modeling under cyclic loading, University of Wollongong, Australia

27. Sol-Sa´nchez M, Thom NH, Moreno-Navarro F, Rubio-gamez MC, Airey GD (2015) A study into the use of crumb rubber in railway ballast. Constr Build Mater 75**:**19-24. http://dx.doi.org/10.1016/j.conbuildmat.2014.10.045

28. Song W, Huang B, Shu X, Wu H, Gong H, Han B, Zou J (2019) Improving damping properties of railway ballast by addition of tire-derived aggregate. Transp Res Re 2673**:**299-307. https://doi.org/10.1177/0361198119839345

29. Suiker ASJ (2002) The mechanical behaviour of ballasted railway tracks. Delft University Press, Netherlands